

Estimation of area-average sensible heat flux using a large-aperture scintillometer during the Semi-Arid Land-Surface-Atmosphere (SALSA) experiment

A. Chehbouni,^{1,2} Y. H. Kerr,³ C. Watts,⁴ O. Hartogensis,⁵ D. Goodrich,⁶ R. Scott,⁷ J. Schieldge,⁸ K. Lee,⁷ W. J. Shuttleworth,⁷ G. Dedieu,³ and H. A. R. De Bruin⁵

Abstract. The use of a large-aperture scintillometer to estimate sensible heat flux has been successfully tested by several investigators. Most of these investigations, however, have been confined to homogeneous or to sparse with single vegetation-type surfaces. The use of the scintillometer over surfaces made up of contrasting vegetation types is problematic because it requires estimates of effective roughness length and effective displacement height in order to derive area-average sensible heat from measurements of the refractive index. In this study an approach based on a combination of scintillometer measurements and an aggregation scheme has been used to derive area-average sensible heat flux over a transect spanning two adjacent and contrasting vegetation patches: grass and mesquite. The performance of this approach has been assessed using data collected during the 1997 Semi-Arid Land-Surface-Atmosphere field campaign. The results show that the combined approach performed remarkably well, and the correlation coefficient between measured and simulated area-average sensible heat flux was ~ 0.95 . This is of interest because this approach offers a reliable means for validating remotely sensed estimates of surface fluxes at comparable spatial scales.

1. Introduction

The turbulent heat fluxes near the ground surface are strongly affected by the ability of the surface to redistribute the radiative energy absorbed from the Sun and the atmosphere into sensible and latent heat. These fluxes play a key role in regulating the energy balance of the atmosphere, which in turn drives atmospheric circulation. For this reason, recent efforts have concentrated on improving the parameterization of land-surface processes in atmospheric models by taking into account the effect of surface heterogeneities on the exchanges processes [Avisar, 1995]. The problem, however, is the difficulty in validating model simulations at regional and certainly at the global circulation model (GCM) scale. On the other hand, it is necessary to validate GCM output because unless these models can reliably simulate the observed water and energy cycles in the present climate, future predictions of climate change are

rather tenuous [Kinter and Shukla, 1990]. To address this issue, the international community has coordinated several multidisciplinary field experiments for collecting hydrologic, atmospheric, and remote sensing data over a range of spatial and temporal scales. One of the unique features of these field experiments has been the deployment of a network of several single-point measurements of surface fluxes, i.e., eddy correlation or Bowen ratio stations for validating atmospheric and hydrologic models. There are technical limitations on using such systems related to the required horizontal homogeneity of the surface layer, the expensive, and the training [De Bruin et al., 1995].

Several investigations recently demonstrated the potential of using scintillometers to obtain areally averaged sensible heat fluxes over path lengths of several kilometers, which are similar to satellite measurement scales [Wesely and Derzko, 1975; Wesely, 1976a, b; Kohsiek, 1985, 1987; De Bruin et al., 1995; McAneney et al., 1995; Green et al., 1994; Lagouarde et al., 1996; Hartogensis, 1997]. The scintillation method works by transmitting a beam of electromagnetic radiation and measuring the intensity variations of the received signal. This leads to a direct measure of the strength of the refractive index of the air and then to the structure parameter for the refractive index (C_n^2), which can then be related to the structure function parameter of temperature (C_T^2) used to derive sensible heat flux.

The objective of this study is to use a large-aperture scintillometer (LAS) to estimate areally averaged sensible heat flux over a transect made up of two adjacent patches (a grass-covered patch and a primarily mesquite-covered patch) with contrasting water status and roughness length. Scintillometer-based sensible heat flux is compared to a weighted average of those measured over each individual patch using two independent three-dimensional eddy correlation systems. The experiment took place in the San Pedro Basin within the context of

¹Institut de Recherche pour le Développement/Instituto del Medio Ambiente y Desarrollo Sustentable, Reyes and Aguascalientes Esq., Hermosillo, Mexico.

²Permanently at Institut de Recherche pour le Développement, Paris, France.

³Le Centre d'Etudes Spatiales de la Biosphère, Toulouse, France.

⁴Instituto del Medio Ambiente y Desarrollo Sustentable, Hermosillo, Mexico.

⁵Department of Meteorology, Wageningen Agricultural University, Wageningen, Netherlands.

⁶Agricultural Research Service, United States Department of Agriculture, Tucson, Arizona.

⁷Department of Hydrology and Water Resources, University of Arizona, Tucson.

⁸Jet Propulsion Laboratory, California Institute of Technology, Pasadena.

the Semi-Arid Land-Surface-Atmosphere (SALSA) research program [Goodrich *et al.*, 1998].

2. Physical Background

2.1. Theoretical Principles

In a turbulent medium such as the Earth's atmosphere the turbulent refractive index fluctuations η are affected by fluctuation of temperature, humidity, and pressure. However, the contribution of atmospheric pressure fluctuation to the refractive index is known to be small, and its effect can be neglected [Hill, 1989]. According to Andreas [1989] the refractive index fluctuation η is related to temperature T' and humidity q' fluctuations, thus

$$\eta = A_T(\lambda, P, T, q) \frac{T'}{T} + A_q(\lambda, P, T, q) \frac{q'}{q} \quad (1)$$

where A_T and A_q are known functions that depend on the optical wavelength λ , the total atmospheric pressure P , the air temperature T , and the specific humidity, q . In the visible and near-infrared region of the electromagnetic spectrum the dependence of A_T and A_q on λ is very small. For $\lambda = 0.94 \mu\text{m}$, which is the wavelength of the scintillometer used in this study, these functions can be parameterized following Andreas [1989] as

$$A_T = -0.78 \times 10^{-6} \frac{P}{T} \quad (2)$$

$$A_q = -57.22 \times 10^{-6} q \quad (3)$$

The refractive index fluctuations η in a turbulent medium are a random function of time t and position x . In turbulence theory it is common to describe the spatial variability or "structure" of a variable by the so-called structure function $D_A(r)$ [Panofsky and Dutton, 1984]. The structure function of refractive index fluctuations η for separation distances r in the inertial subrange of scales about a point x is

$$D_n(r) = [\overline{\eta(x) - \eta(x+r)}]^2 = C_n^2 r^{2/3} \quad l_0 < r < L_0 \quad (4)$$

where C_n^2 is the refractive index structure parameter representing the amplitude of the variations in the refractive index and the overbar denotes a time or ensemble average [Lagouarde *et al.*, 1996]. The inertial subrange for which (4) is valid is the range in the turbulent spectrum in which turbulent energy is transferred from larger to smaller wavelengths. The inner scale l_0 marks the transition between the inertial and viscous energy dissipating range of eddy sizes and is of the order of 0.5–1.0 cm near the surface. The integral or outer scale L_0 describes the scale of the dominant inhomogeneities, which is of the order of half the height of measurement above the surface.

On the basis of Tatarskii's [1961] theory, Clifford *et al.* [1974] showed that for a LAS the variance of the natural logarithm of the irradiance I incident at the receiver is

$$\sigma_{\ln(I)}^2 = \overline{[\ln(I) - \overline{\ln(I)}]^2} = \int_0^1 C_n^2(u) W(u) du \quad (5)$$

where $W(u)$ is a spatial weighing function given by

$$W(u) = 16\pi^2 k^2 L \int_0^\infty dK K \Phi_n(K) \sin^2 [K^2 L u (1-u)/2k] \cdot [2J_1(x_1)2J_1(x_2)/(x_1 x_2)]^2 \quad (6)$$

$u = x/L$ is the normalized pathlength; L is the path length; $k = 2\pi/\lambda$ is the optical wave number; $x_1 = KD_R u/2$ and $x_2 = KD_T u/2$, where D_R and D_T are the receiver and transmitter apertures, respectively; K is the three-dimensional spatial wave number; J_1 is a Bessel function of the first kind of order one; and Φ_n , the three-dimensional Kolmogorov spectrum of the refractive index, describes the turbulent medium in terms of its Fourier components K :

$$\Phi_n(K) = 0.033 C_n^2 K^{-11/3} \quad (7)$$

After integrating (6) and using (5) and (7), Wang *et al.* [1978] obtained

$$C_n^2 = C \sigma_{\ln(I)}^2 (D_R/D_T)^{7/3} L^{-3} \quad (8)$$

where C is a calibration constant, which is a function of the ratio D_R/D_T . For equal receiver and transmitter apertures, as is the case here, C_n^2 can be described as a linear function of $\sigma_{\ln(I)}^2$ measured by the scintillometer as

$$C_n^2 = C \sigma_{\ln(I)}^2 D^{7/3} L^{-3} \quad (9)$$

where $C = 1.12$ for C_n^2 ranges from 10^{-17} to $10^{-12} \text{ m}^{-2/3}$ and D is the diameter of the receiver/transmitter.

2.2. Sensible Heat Flux

A scintillometer is an instrument that measures the intensity of a light beam fluctuation after propagating through a turbulent medium. It is assumed that these intensity fluctuations are caused by inhomogeneities in the refractive index, which are due to turbulent eddy motions along the scintillometer path. The eddy motions are generated by temperature and humidity fluctuations and can be regarded as a collection of converging and diverging lenses focusing and defocusing the scintillometer beam [McAneney *et al.*, 1995]. In the visible and infrared region, assuming that temperature and humidity fluctuations are perfectly correlated, the spatially averaged refractive index structure parameter measured directly by a LAS is related to the temperature structure parameter as

$$C_T^2 = C_n^2 \left(\frac{T^2}{-0.78 \times 10^{-6} P} \right)^2 \left(1 + \frac{0.03}{\beta} \right)^{-2} \quad (10)$$

where β is the Bowen ratio that is incorporated as a humidity correction such that C_T^2 decreases with increasing evaporation rate. The study by De Wekker [1996] showed that this term can be neglected whenever the Bowen ratio is >0.6 , which is generally the case over natural surfaces in arid and semiarid areas. The sensible heat and momentum fluxes together determine atmospheric stability, and this in turn influences turbulent transport, thus an iterative procedure is needed to calculate sensible heat flux from the scintillometer measurement [Lagouarde *et al.*, 1996].

We first define the dimensionless temperature scale θ^* as

$$\theta^* = H/\rho c_p u^* \quad (11)$$

where ρ is the density of the air, c_p is the heat capacity at constant pressure, and u^* is the friction velocity given from

$$u^* = \frac{ku}{\ln\left(\frac{z-d}{z_0}\right) - \psi_m\left(\frac{z_0-d}{L_{\text{mon}}}\right)} \quad (12)$$

where z is the measurement height, z_0 is the roughness length, d is the displacement height, ψ_m is the integrated stability function, and L_{mon} is the Monin-Obukhov length defined as

$$L_{\text{mon}} = \frac{Tu_*^2}{kg\theta_*} \quad (13)$$

Under unstable conditions, *De Bruin et al.* [1993, 1995] found that the temperature structure parameter C_T^2 and θ^* are related by

$$\frac{C_T^2(z-d)^{2\beta}}{\theta_*^2} = 4.9 \left(1 - 9 \frac{z-d}{L_{\text{mon}}}\right)^{-2\beta} \quad (14)$$

Sensible heat flux can then be derived using (10)–(14) via iteration.

2.3. Derivation of Area-Average Sensible Heat Flux Over Patchy Surfaces

Inferring area-average sensible heat flux using scintillometer from (10)–(14) requires an aggregation rule that allows for the derivation of effective value of the roughness length z_0 and the displacement height d . This is a classical “aggregation problem,” where a link needs to be established between the relevant parameters at the patch scale and at the grid scale. Fortunately, there has been substantial progress in specifying area-average parameters using either empirical [*Mason, 1988; Blyth et al., 1993; Blyth and Harding, 1995; Noilhan and Lacarrere, 1995; Shuttleworth, 1988, 1991; Arain et al., 1996*] or theoretical approaches [*Lhomme, 1992; Lhomme et al., 1994; Chehbouni et al., 1995; Raupach, 1991, 1995; Raupach and Finnigan, 1995*]. Following *Shuttleworth et al.* [1997], effective roughness length can be formulated as

$$\ln^{-2}\left(\frac{z_b-d}{z_0}\right) = \sum_i w_i \ln^{-2}\left(\frac{z_b-d_i}{z_{oi}}\right) \quad (15)$$

while the effective displacement height can be formulated as

$$d = \sum_i w_i d_i \quad (16)$$

where z_{oi} and d_i are the patch scale roughness length and displacement height, respectively, which were derived as functions of the vegetation height; w_i is the fraction of the surface covered by the patch i ; and z_b is the blending height, which is expressed as a function of the friction velocity, wind speed, and horizontal length scale [*Wieringa, 1986*].

3. Experiment

3.1. Site Description

This study took place in the Upper San Pedro Basin (USPB), which represents the focus study region for the SALSA program. The basin originates in northern Sonora, Mexico, and flows north into southeast Arizona. (see Figure 1 for site location). The basin embodies a number of characteristics that make it an exceptional outdoor laboratory for addressing a large number of scientific challenges in arid and semiarid hydrology, meteorology, ecology, and social and pol-

icy science [*Goodrich et al., 1998*]. The basin is a transition area between the Sonoran and Chihuahuan Deserts. It is an international basin spanning the Mexico-United States border with significantly different cross-border legal and land-use practices, significant topographic and vegetation variation, and a highly variable climate. The annual rainfall ranges from ~300 to 750 mm, with the majority of annual precipitation (~65%) occurring during the July through September monsoon season from high-intensity convective thunderstorms and ~30% coming from less intense winter frontal systems. Major vegetation types include desert shrub-steppe, grasslands, oak savannah, pinyon-juniper, and ponderosa pine. For this study an experimental site made up of two adjacent patches (i.e., a sacaton grass site adjacent to a mixed mesquite/grassland site) on the San Pedro River flood plain was chosen. The aerodynamic characteristics of the two patches were very different: the grass was ~1 m in height, and the mesquite was ~3.5 m in height.

3.2. Instrumentation

During the monsoon period, measurements include basic meteorological data, i.e., wind speed and direction at different heights, incoming radiation, air temperature, and humidity. Additionally, soil moisture, vegetation sampling, and surface reflectance and temperature were also taken. Fluxes of sensible heat and water vapor were measured above both grass and the mesquite patches using an eddy covariance-based method. Over the grass patch the eddy covariance station consisted of a three-dimensional sonic anemometer and krypton hygrometer manufactured by Campbell Scientific, Inc. Over the mesquite patch the eddy covariance system comprises a three-axis sonic anemometer manufactured by Gill instrument (Solent A1012R) and an IR gas analyzer (LI-COR 6262 model), which was used in close path mode. The system is controlled by specially written software that calculates the surface fluxes of momentum, sensible and latent heat, and carbon dioxide from the output of the sonic and IR gas analyzer and displays them in real time. During the first portion of the campaign an inter-comparison of flux instruments was conducted over a homogeneous region of the sacaton grass.

The LAS used in this study was designed and built at the Department of Meteorology of the Wageningen Agricultural University, and the electronics are those described by *Ochs and Wilson* [1993]. The LAS has an aperture size of 0.15 m, and the light source is a light-emitting diode (LED: TIES-16A, Texas Instruments), operating at a peak wavelength of 0.94 μm , placed at the focal point of a concave mirror (see Figure 2 for a picture of the LAS). The reflected beam emitted by the transmitter diverges slightly (by ~0.002°). The irradiance distribution over the beam is completely uniform. The receiver employs an identical mirror to focus light on a photo diode detector. To distinguish the light emitted by the LAS from ambient radiation, it is excited by a 7 kHz square wave. Scintillations appear as amplitude modulations on the carrier wave. For beam alignment, telescope rifle sights are mounted on both the receiver and emitter housings.

In this study the receiver and the emitter were ~900 m apart, spanning a transect made up of 25% grass and 75% mixed mesquite and grass. The average measurement height was 10.5 m above the soil surface. The receiver electronics are designed in such a way that after setting the path length it gives an output voltage such that C_n^2 can be derived from $C_n^2 = 10^{(V_{\text{out}}-12)}$, where V_{out} is the output voltage of the scintillometer. Ten minute average values of the scintillometer output

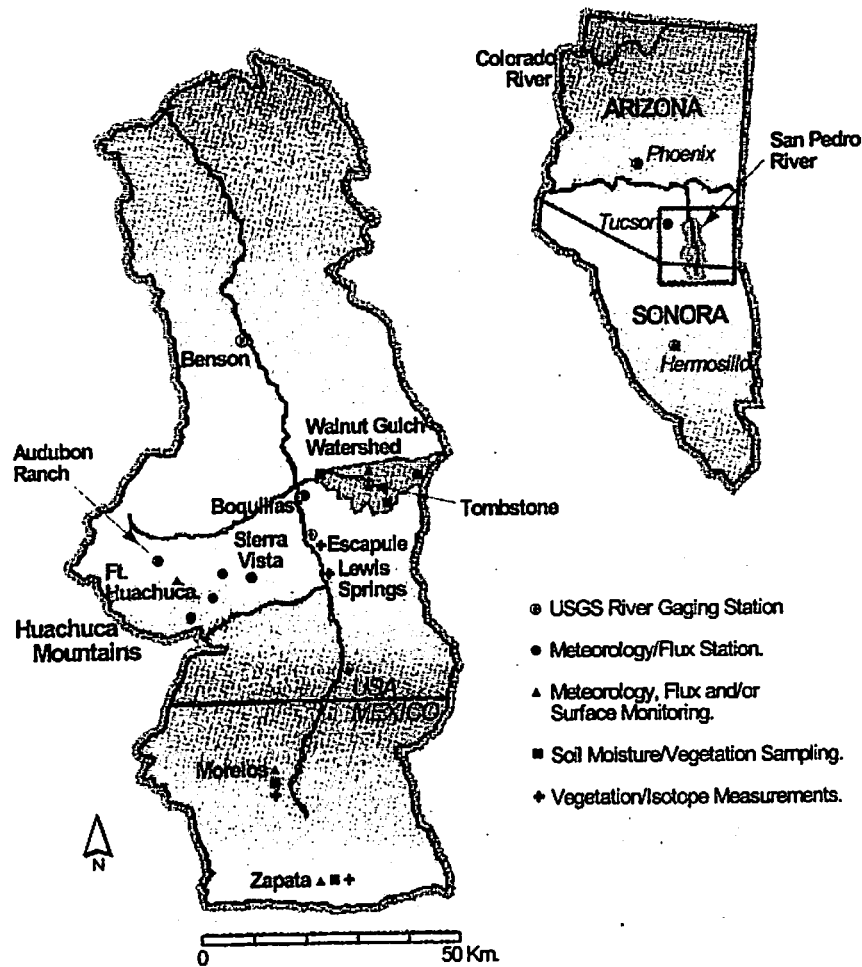


Figure 1. Location map of the Upper San Pedro Basin.

V_{out} were stored on a data logger (Campbell Scientific, Inc., 21X). These data were linearly averaged to provide 30 min average values.

4. Results

4.1. Intercomparison of Measurement Systems

During the first part of the intensive campaign, two eddy correlation instruments were deployed next to each other over

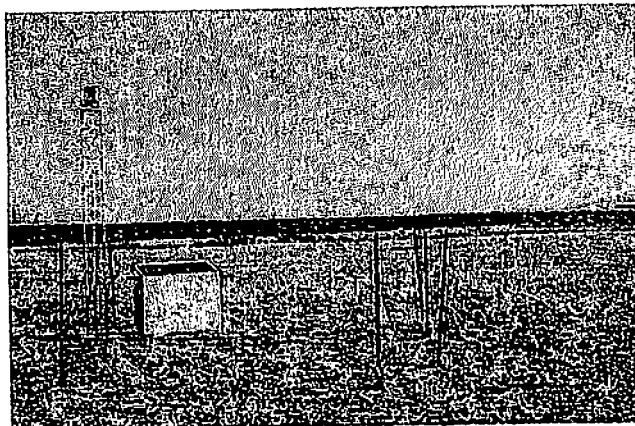


Figure 2. Picture of the emitter of the large-aperture scintillometer (the receiver looks similar).

a homogeneous sacaton grass. At the same time the scintillometer was installed over the same patch, sampling a transect of ~300 m corresponding to the footprint of the eddy correlation instruments. In Figure 3a, sensible heat flux estimated by the scintillometer is compared to the values obtained using the

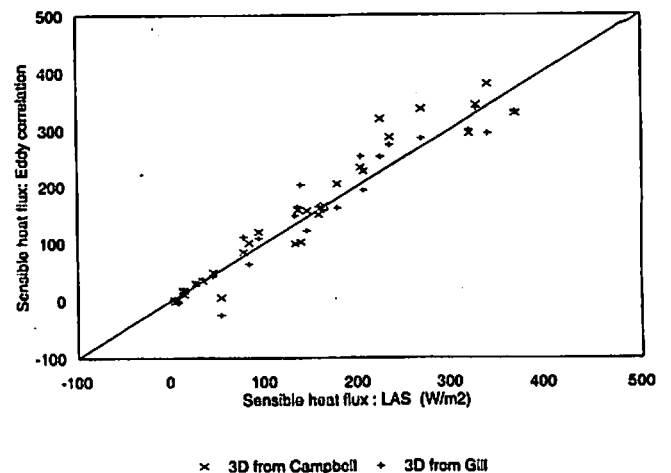


Figure 3a. Comparison between sensible heat flux obtained with the scintillation method and the corresponding values measured with eddy correlation systems during the intercomparison period: Gill, pluses, and Campbell, crosses.

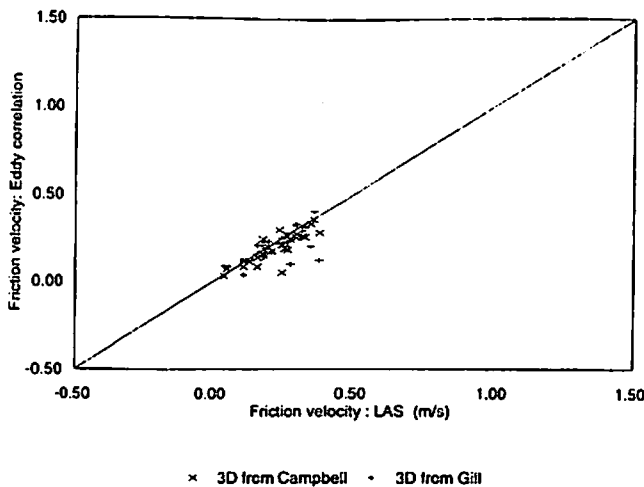


Figure 3b. Comparison between friction velocity with the scintillation method and the corresponding values measured with eddy correlation systems during the intercomparison period: Gill, pluses, and Campbell, crosses.

eddy correlation instruments. Figure 3b presents the same comparison for friction velocity. It is seen that except for a few outliers the correspondence is good. The differences between the scintillometer and eddy correlation estimates for both sensible heat flux and friction velocity are of the same magnitude as the difference between the two eddy correlation systems. The statistical results comparing the different systems are given in Table 1a for sensible heat flux and in Table 1b for the friction velocity. This confirms the result obtained elsewhere [De Bruin et al., 1996; Lagouarde et al., 1996], where comparisons of sensible heat flux measured by the scintillometer and eddy correlation over short distances are within experimental error. Therefore no adjustment of the two eddy correlation measurements has to be made.

After the intercalibration period one of the eddy correlation systems (Gill) was deployed over the mesquite patch, while the other (Campbell) was deployed over the grass patch. At the same time the transmitter and the receiver of the scintillometer were set ~900 m apart to sample a transect made up of 75% mesquite and 25% grass. Figures 4a and 4b present the difference in measured sensible heat flux and friction velocity between the grass and mesquite patches. Figures 4a and 4b demonstrate that there are significant differences between the two patches, which can be up to 150 W m⁻² for sensible heat flux and 0.5 m s⁻¹ for *u**. This contrasted behavior can be ex-

Table 1a. Statistical Results of the Intercomparison Between the Sonic From Campbell, the Sonic from Gill, and the Large Aperture Scintillometer (LAS) in Estimating Sensible Heat Flux

	N	MAD	RMSD	X _{coeff}	R ²	Const
Gill/Campbell	29	23.04	34.89	1.04	0.92	1.59
Gill/LAS	29	20.88	28.40	0.95	0.94	5.34
Campbell/LAS	29	22.64	31.63	0.88	0.94	8.86

N is the number of observations; MAD is the mean absolute difference; RMSD is the Root Mean Square Difference; X_{coeff} is the slope of the linear regression; R² is the correlation coefficient; and Const is the constant of linear regression.

Table 1b. Statistical Results of the Intercomparison Between the Sonic From Campbell, the Sonic from Gill, and the LAS in Estimating Friction Velocity

	N	MAD	RMSD	X _{coeff}	R ²	Const
Campbell/LAS	29	0.04	0.06	0.89	0.70	0.88
Gill/Campbell	29	0.05	0.07	0.62	0.39	1.04
Gill/LAS	29	0.05	0.07	0.71	0.45	0.95

plained by the difference in terms of the canopy height and the root system depth between the grass and the mesquite. These parameters greatly influence the aerodynamic flow above the canopy and the partitioning of available energy into sensible latent heat flux.

4.2. Validation and Discussion

Equations (10)–(14) were used in conjunction with effective roughness length and effective displacement height obtained from (15) and (16) to derive area-average sensible heat flux and friction velocity using scintillometer measurements taken under unstable conditions from days of the year (DOYs) 225–231. To verify the performance of the scintillometer, it is necessary to derive an area-average friction velocity and area-average sensible heat flux from eddy correlation measurements independently from each patch.

Simple weighted averages of the fluxes measured by the three-dimensional sonics over the grass and the mesquite patches were used for the area-average sensible heat flux. However, estimating area-average friction velocity is not trivial. The approach adopted here was to obtain area-average momentum flux ($\rho u^*{}^2$) as a weighted average of the fluxes measured independently over each patch and then match it with that formulated in terms of effective friction velocity. This leads to the following relationship between effective friction velocities *u** and components friction velocities *u**_i:

$$u^* = \left(\sum_i w_i u_i^{*2} \right)^{0.5} \tag{17}$$

Figure 5 presents a comparison between the scintillometer-based friction velocity and that obtained using (17) in conjunction with measured component friction velocities. The scatter

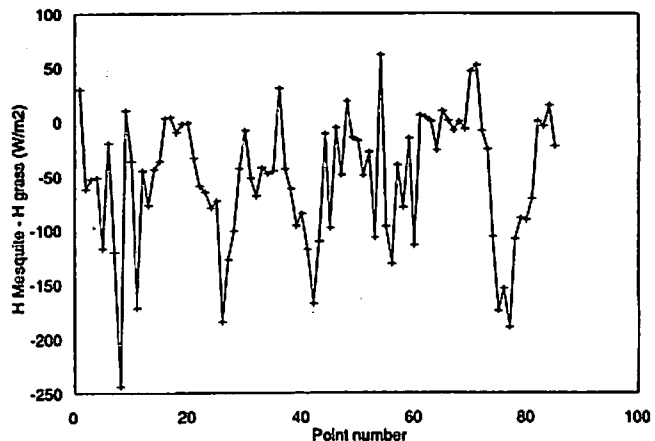


Figure 4a. Differences of sensible heat flux measured over mesquite and over grass.

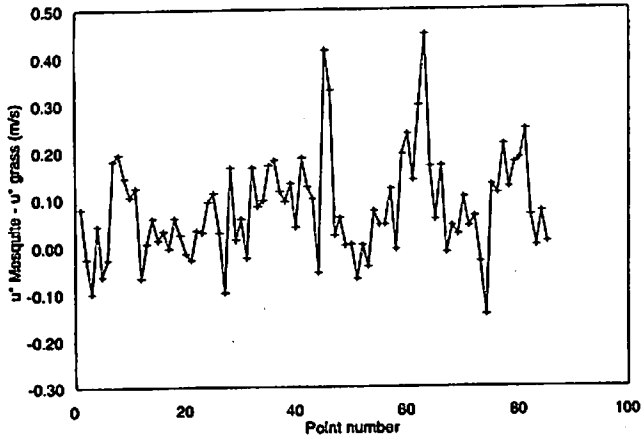


Figure 4b. Differences of friction velocity measured over mesquite and over grass.

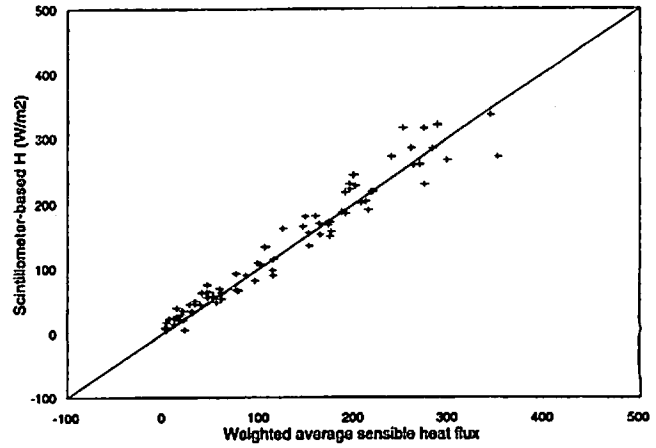


Figure 6. Comparison between measured area-average sensible heat flux and the corresponding values derived from the scintillometer measurements.

in Figure 5 is larger than those reported in the literature. However, it is important to remember that this study is for a very complex surface where heterogeneity is present at both patch and grid scales. Figure 6 presents a comparison between measured values of area-average sensible heat flux and the corresponding values estimated by the scintillometer. The correspondence between the two are very good. Statistical analysis of the performance of the LAS in estimating area-average H and u^* are presented in Table 2. The performance of the scintillometer in estimating area-average sensible heat flux over contrasting patches in this study is very similar to that reported over a single patch [McAneney *et al.*, 1995]. This suggests the robustness of the scintillometer approach over nonuniform surfaces.

This result is very encouraging because it suggests that reliable area-average estimates of sensible heat flux can be obtained to validate large-scale atmospheric models without the need to deploy a network of hydrometeorological devices such as eddies. However, a number of issues need to be addressed before it is possible to generalize the results obtained in this study. As can be seen from (10), estimating C_T^2 from C_n^2 requires a humidity correction factor that has been legitimately

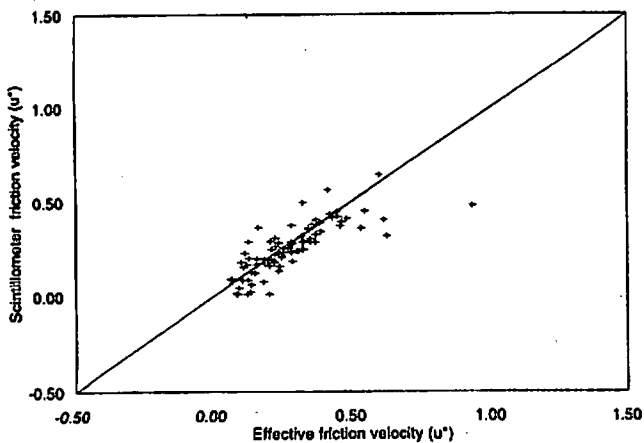


Figure 5. Comparison between effective friction velocity derived from eddy correlation measurements and the corresponding values evaluated with the scintillometer. Units are $m s^{-1}$.

neglected here. This is not necessarily always the case. The problem arises when the scintillometer measurements are made over transects that comprised several patches with significantly different evaporating rates (and different low Bowen ratios). In this case it is necessary to derive an effective Bowen ratio, and this may not be trivial. Additionally, there is a need to investigate the case where the sign of the heat flux changes along the transect because the scintillometer cannot distinguish between stable and unstable conditions. Finally, the issue associated with changes in wind direction from downpath to cross-path needs to be investigated.

5. Conclusions

Several successful studies have investigated the use of the scintillometer in estimating area-average sensible heat flux over homogeneous surfaces. The objective of this study was to test the performance of the scintillometer over a surface made up of two contrasting patches. The approach used was to combine scintillometer measurements with an aggregation scheme to derive effective roughness length and effective displacement. The result showed that the agreement between the measured and simulated area-average sensible heat flux values is very good. The LAS has several major advantages for measuring sensible heat flux: (1) it is not sensitive to flow distortions near the instrument; (2) it is easy to operate and to maintain; (3) it gives statistically more reliable data, which allowed for averaging over a short time period. More importantly, it can provide a reliable tool for estimating sensible heat flux at spatial scales compatible with meteorological models and remote-sensing satellites.

Table 2. Statistical Results of the Comparison Between Measured and Scintillometer-Based Area-Average Sensible and Friction Velocity

	N	MAD	RMSD	X_{coeff}	R^2	Const
Sensible heat flux	84	16.9	22.5	0.97	0.95	11.10
Friction velocity	84	0.06	0.10	0.62	0.63	0.06

Acknowledgments. We acknowledge financial support from CONACYT, the French remote sensing program PNTS, and the European Commission and ESA through VEGETATION and ERS2/ATSR2 projects. This research is situated within the framework of NASA Mission to Planet Earth (MTPE): NASA/EOS grant NAGW2425. Additional support was also provided by the USDA-ARS Global Change Research Program and NASA grant W-18-1997. Many thanks to ARS-Tombstone staff for helping during the course of the experiment and to B. Heusinkveld from WAU for his help during the processing of the scintillometer data. We are thankful to C. Thies and F. Santiago for their editorial assistance.

References

- Andreas, E. L., Two-wavelength method of measuring path-averaged turbulent surface heat fluxes, *J. Atmos. Oceanic Technol.*, **6**, 280–292, 1989.
- Arain, A. M., J. D. Michaud, W. J. Shuttleworth, and A. J. Dolman, Testing of vegetation parameter aggregation rules applicable to the Biosphere-Atmosphere Transfer Scheme (BATS) at the FIFE site, *J. Hydrol.*, **50**, 3751–3774, 1996.
- Avisar, R., Scaling of land-atmosphere interactions, an atmospheric modelling perspective, *Hydrol. Processes*, **9**, 679–695, 1995.
- Blyth, E. M., and R. J. Harding, Application of aggregation models to surface heat flux from Sahelian tiger bush, *Agric. For. Meteorol.*, **72**, 213–235, 1995.
- Blyth, E. M., A. J. Dolman, and N. Wood, Effective resistance to sensible and latent heat flux in heterogeneous terrain, *Q. J. R. Meteorol. Soc.*, **119**, 423–442, 1993.
- Chehbouni, A., E. G. Njoku, J.-P. Lhomme, and Y. H. Kerr, An approach for averaging surface temperature and surface fluxes over heterogeneous surfaces, *J. Clim.*, **5**, 1386–1393, 1995.
- Clifford, S. F., G. R. Ochs, and R. S. Lawrence, Saturation of optical scintillation of strong turbulence, *J. Opt. Soc. Am.*, **64**, 148–154, 1974.
- De Bruin, H. A. R., W. Kohsiek, and B. J. J. M. van den Hurk, A verification of some methods to determine the fluxes of momentum, sensible heat, and water vapour using standard deviation and structure parameter of scalar meteorological quantities, *Boundary Layer Meteorol.*, **63**, 231–257, 1993.
- De Bruin, H. A. R., B. J. J. M. van den Hurk, and W. Kohsiek, The scintillation method tested over a dry vineyard area, *Boundary Layer Meteorol.*, **76**, 25–40, 1995.
- De Bruin, H. A. R., J. P. Nieveen, S. F. J. de Wekker, and B. G. Heusinkveld, Large aperture scintillometry over a 4.8 km path for measuring areally-averaged sensible heatflux, paper presented at 22nd AMS Symposium on Agricultural and Forest Meteorology, Am. Meteorol. Soc., Atlanta, Ga., 1996.
- De Wekker, S. F. J., The estimation of areally-averaged sensible heat fluxes over complex terrain with a large-aperture scintillometer, M.S. thesis, Dep. of Meteorol., Wageningen Agric. Univ., Wageningen, Neth., 1996.
- Goodrich, D. C., et al., An overview of the 1998 activities of the Semi-Arid Land-Surface Program, paper presented at 1998 American Meteorological Society Meeting, Phoenix, Ariz., 1998.
- Green, A. E., K. J. McAneney, and M. S. Astill, Surface-layer scintillation measurements of daytime sensible and momentum fluxes, *Boundary Layer Meteorol.*, **68**, 357–373, 1994.
- Hartogensis, O., Measuring areally-averaged sensible heat fluxes with a large aperture scintillometer, M.S. Thesis, Dep. of Meteorol., Wageningen Agricultural University, Wageningen, Neth., 1997.
- Hill, R. J., Implications of Monin-Obukhov similarity theory for scalar quantities, *J. Atmos. Sci.*, **6**, 2236–2244, 1989.
- Kinter, J. L., and J. Shukla, The global hydrologic and energy cycles: Suggestions for studies in pre-global energy and water cycle experiment (GEWEX) period, *Bull. Am. Meteorol. Soc.*, **71**, 181–189, 1990.
- Kohsiek, W., A comparison between line-averaged observations of C_n^2 from scintillation of a CO₂ laser beam and time averaged in situ observations, *J. Clim. Appl. Meteorol.*, **24**, 1099–1102, 1985.
- Kohsiek, W., A 15 cm aperture LED scintillometer for C_n^2 and cross-wind measurements, *KNMI Sci. Rep. WR 87-3*, Royal Neth. Meteorol. Inst., DeBilt, 1987.
- Lagouarde, J.-P., K. J. McAneney, and E. F. Green, Scintillometer measurements of sensible heat flux over heterogeneous surfaces, in *Scaling Up in Hydrology Using Remote Sensing*, edited by J. B. Stewart et al., pp. 147–160, John Wiley, New York, 1996.
- Lhomme, J. P., Energy balance of heterogeneous terrain: Averaging the controlling parameters, *Agric. For. Meteorol.*, **61**, 11–21, 1992.
- Lhomme, J. P., A. Chehbouni, and B. Monteny, Effective parameters of surface energy balance in heterogeneous landscape, *Boundary Layer Meteorol.*, **71**, 297–309, 1994.
- Mason, P. J., The transformation of areally-averaged roughness lengths, *Q. J. R. Meteorol. Soc.*, **114**, 399–420, 1988.
- McAneney, K. J., A. E. Green, and M. S. Astill, Large aperture scintillometry: The homogenous case, *Agric. For. Meteorol.*, **76**, 149–162, 1995.
- Noilhan, J., and L. Lacarrere, GCM gridscale evaporation from mesoscale modelling: A method based on parameter aggregation tested for clear days of Hapex-Mobilhy, *J. Clim.*, **8**, 206–223, 1995.
- Ochs, G. R., and J. J. Wilson, A second-generation large-aperture scintillometer, *NOAA Tech. Memo. ERL WPL-232*, NOAA Environ. Res. Lab., Boulder, Colo., 1993.
- Panofsky, H. A., and J. A. Dutton, Atmospheric turbulence, in *Models and Methods for Engineering Applications*, 397 pp., John Wiley, New York, 1984.
- Raupach, M. R., Vegetation-atmosphere interaction in homogeneous and heterogeneous terrain: Some implications of mixed-layer dynamics, *Vegetatio*, **91**, 105–120, 1991.
- Raupach, M. R., Vegetation-atmosphere interaction and surface conductance at leaf, canopy and regional scales, *Agric. For. Meteorol.*, **73**, 151–179, 1995.
- Raupach, M. R., and J. J. Finnigan, Scale issues in boundary-layer meteorology: Surface energy balances in heterogeneous terrain, *Hydrol. Processes*, **9**, 589–612, 1995.
- Shuttleworth, W. J., Macrohydrology: The new challenge for process hydrology, *J. Hydrol.*, **100**, 31–56, 1988.
- Shuttleworth, W. J., The modellion concept, *Rev. Geophys.*, **29**, 585–606, 1991.
- Shuttleworth, W. J., Z.-L. Yang, and M. A. Arain, Aggregation rules for surface parameters in global models, *Hydrol. Earth Syst. Sci.*, **1**, 217–226, 1997.
- Tatarskii, V. I., Wave propagation in a turbulent medium, 285 pp., McGraw-Hill, New York, 1961.
- Wang, T. I., G. R. Ochs, and S. F. Clifford, A saturation-resistant optical scintillometer to measure, *J. Opt. Soc. Am.*, **69**, 334–338, 1978.
- Wesely, M. L., The combined effect of temperature and humidity on the refractive index, *J. Appl. Meteorol.*, **15**, 43–49, 1976a.
- Wesely, M. L., A comparison of two optical methods for measuring line-averages of thermal exchanges above warm water surfaces, *J. Appl. Meteorol.*, **15**, 1177–1188, 1976b.
- Wesely, M. L., and Z. I. Derzko, Atmospheric turbulence parameters from visual resolution, *Appl. Opt.*, **14**, 847–853, 1975.
- Wieringa, J., Roughness dependent geographical interpolation of surface wind speed averages, *Q. J. R. Meteorol. Soc.*, **112**, 867–889, 1986.
- A. Chehbouni, IRD/IMADES, Reyes and Aguascalientes Esq., Col. San Benito, Hermosillo CP 83190, Sonora, Mexico. (ghani@cideson.mx)
- H. De Bruin and O. Hartogensis, Department of Meteorology, Wageningen Agricultural University, Duivendaal 2, 6701 AP Wageningen, bodnummer 4, Netherlands.
- G. Dedieu and Y. H. Kerr, CESBIO, 31055 Toulouse, France.
- D. Goodrich, Agricultural Research Service, United States Department of Agriculture, Tucson, AZ 85719.
- K. Lee, R. Scott, and W. J. Shuttleworth, Department of Hydrology and Water Resources, University of Arizona, Tucson, AZ 85721.
- J. Schiedge, Jet Propulsion Laboratory, California Institute of Technology, Pasadena, CA 91109-8099.
- C. Watts, IMADES, Hermisillo CP 83190, Sonora, Mexico.

(Received August 3, 1998; revised March 29, 1999; accepted March 31, 1999.)